

Synthesis, Structure, NMR Spectroscopy, and Electrochemistry of the Sterically Congested Triarylar sine Dipp₃As: EPR Characterization of its Radical Cation

Mona Taghavikish,^A Brock L. Price,^A Tracey L. Roemmele,^A and René T. Boere^{A,B}

^ADepartment of Chemistry and Biochemistry, University of Lethbridge, Lethbridge, Alberta, T1K3M4, Canada.

^BCorresponding author. Email: boere@uleth.ca

The synthesis, NMR spectroscopy, single-crystal X-ray structure, and solution electrochemistry of the new compound [2,6-{CH(CH₃)₂C₆H₃]₃As, abbreviated as Dipp₃As, is reported. The molecule, prepared by reaction of AsCl₃ with a pre-formed aryl copper reagent, Dipp₄Cu₄, crystallizes in the hexagonal space group *R*3̄ as a racemic twin. The sum of angles around As, $\sum \angle \{CAsC\}$, is 329.13(3)° in the X-ray structure and 329.17° from an R-B3LYP/6-31G(d,p) hybrid density functional theory calculation. The aromatic rings are quite distorted with both the *ipso* carbon and especially the As atom significantly out of plane by 0.503(3) Å. The ambient temperature NMR spectrum fits for C₃ symmetry implying that inversion is slow on the NMR timescale. Cyclic voltammetry on a glassy carbon electrode in CH₂Cl₂ with 0.4 M [¹⁸Bu₄N][PF₆] over scan rates of 0.05–0.8 V s⁻¹ and temperatures of 22 ± 2°C produced one quasi-reversible process with $E_{m1} = +0.43$ V at a scan rate of 0.20 V s⁻¹ and a second irreversible process with a peak potential of +1.45 V (v. Fc⁺⁰). The diffusion coefficient has been measured as 3.3 ± 0.1 × 10⁻⁶ cm² s⁻¹ in CH₂Cl₂ solution containing 0.4 M [¹⁸Bu₄N][PF₆]. Chemical oxidation with AgPF₆ in CH₂Cl₂ in degassed solutions in sealed vessels allowed for recording of characteristic EPR spectra; at 293 K, $a(^{75}\text{As}) = 26.1$ mT and $g = 2.021$. In frozen solution, an almost isotropic spectrum is obtained ($g_{\parallel} = 2.000$ mT and $g_{\perp} = 2.003$ mT) and the hyperfine splitting constants are $a_{\parallel} = 47.9$ and $a_{\perp} = 19.0$ mT, leading to an estimate for the structure being slightly pyramidal with $\sum \angle \{CAsC\} \approx 351^\circ$.

Manuscript received: 7 May 2013.

Manuscript accepted: 11 June 2013.

Published online: 2 August 2013.

Introduction

The most crowded triarylphosphines reported to date, using the criterion of the sums of angles around the central atom $\sum \{ \angle \text{CPC} \}$, are those with three 2,6-diisopropylphenyl substituents, namely Dipp₃P and Tripp₃P, where Dipp = 2,6-diisopropylphenyl and Tripp = 2,4,6-triisopropylphenyl.^[1,2] Interest in the redox properties of this class of compounds is on-going^[3–8] and the first crystal structures of a phosphoniumyl radical cation were recently reported for several salts of Tripp₃P^{+•}.^[9] There is also very strong current interest in the preparation, properties and applications of heavy p-block element radicals,^[10–16] but according to Konu and Chivers in 2010: ‘the chemistry of stable arsenic-, antimony-, and bismuth-centered radicals has remained virtually unexplored’.^[12]

Here we report on the synthesis of a new sterically congested arsine, Dipp₃As, with full characterisation and a thorough examination of its redox properties by chemical and electrochemical methods. The structure was determined by X-ray crystallography at low temperature (LT) which establishes its claim to ‘most sterically congested’ by edging out Tripp₃As^[2] based on the sum of angles metric, $\sum \angle \{CAsC\}$, for flattening at the central atom.^[17] Despite the high steric pressure, the intrinsically greater pyramidal character of arsenic(III) over phosphorus(III) results in a substantially higher barrier to planar

inversion compared with its congener Dipp₃P. Consequently, the solution ¹H NMR spectrum at room temperature (RT) resembles that of the phosphine at –80°C. Another marker of having more pyramidal character is greater stabilisation of the highest occupied molecular orbital (HOMO); this results in a first oxidation potential that is 0.32 V more positive for the arsine compared with Dipp₃P. The steric shielding provided by the bulky Dipp group acts to protect the free radical Dipp₃As^{+•} despite this facile oxidation potential. EPR characterisation in combination with the *I* = 3/2 spin of the 100% abundant ⁷⁵As nucleus provides unambiguous confirmation for the formation of the radical cation and provides a ready handle for monitoring its presence, thereby establishing it as a new *persistent radical*.^[15]

Results and Discussion

Synthesis and Reactions

Dipp₃As is prepared by the reaction of Dipp₄Cu₄ with AsCl₃ in a one-pot reaction starting from DippBr. The use of aryl copper reagents is essential for successful introduction of the third bulky aryl group. If Grignard or lithium reagents are employed in this last step, there is a strong tendency towards reductive coupling rather than substitution (by formation of products such as, for example, Tripp₂P–PTripp₂ from the reaction of PCl₃

with TrippMgBr as shown many years ago by its accidental synthesis).^[18]

Crystal Structure Determinations

The crystal structure of Dipp_3As was determined at low temperature (173 K). A summary of the crystal, structure solution, and refinement data is presented in the Experimental section and selected geometric parameters are compiled in Table 1. The structure can be compared most fruitfully with Tripp_3As reported by Sasaki et al. in 2002 in a short communication.^[2] Similar to Dipp_3P ,^[1] but unlike the related Tripp compounds which have low symmetry space groups, it crystallises as a racemic twin in the chiral space group $R3$ with a 62 : 38 ratio of the two enantiomers defined by C_3 rotation about the principal axis (Fig. 1). The equivalent As–C bonds are 1.9903(9) Å long, compared with an average of 1.986(3) Å in the two independent molecules of the reported structure for Tripp_3As ; these values are not significantly different at the 99% confidence level. The sum of angles around As, $\sum \angle \{\text{CAsC}\} = 329.13(3)^\circ$,^[17] is significantly larger than $\sum \angle \{\text{CAsC}\} = 327.70(4)^\circ$ in Tripp_3As at the 99% confidence level. Similarly, the sum of angles around P in Dipp_3P , $\sum \angle \{\text{CPC}\} = 335.64(2)^\circ$, is larger (even at the 99% confidence level) than that reported around Tripp_3P , 334.4(1)°; whether these effects reflect differences in inductive electron donating ability caused by the ‘extra’ ^iPr group in the Tripp ligands, or are merely due to fortuitous crystal packing effects, remains unclear. There is considerable distortion to the aryl rings due to the severe steric crowding at the central As; for example, whereas the five ring atoms C2 > C6 define a reasonable plane (root mean square (r.m.s.) deviation of 0.005 Å), the *ipso* atom C1 and the As deviate from this plane (in the same direction) by 0.0383(16) and 0.503(3) Å. We note that the sums of the angles at As are 6.5°–6.7° smaller than at P in Dipp_3P , reflecting the higher inherent pyramidalicity of arsenic.^[19] Molecules of Dipp_3As pack densely (Fig. 2) with a single kind of intermolecular contact less than the sum of van der Waals’ radii between an ^iPr methyl hydrogen and a ring carbon atom at 2.870(1) Å. In the chiral space group $R3$, all the $C_3\text{As}$ pyramids are oriented in the same direction (resulting in a high overall polarity); the overall crystal dipole moment is likely reduced as a result of the racemic twinning.

Earlier we introduced the distinction between *steric pressure* and *steric shielding* in $R_3\text{E}$ compounds, where the former refers

to the strong repulsion among the *endo* C10–11–12 isopropyl groups, and the latter to protection by the *exo* C7–8–9 isopropyl groups of the As ‘lone pair’ electrons, which contribute the most to the highest occupied molecular orbital (HOMO) of Dipp_3As .^[1,17] The degree of steric pressure amongst $R_3\text{As}$ species can be ascertained from the aforementioned $\sum \angle \{\text{CAsC}\}$, whereas the degree of steric shielding can be perused visually (Fig. 1) by considering the flanking *exo* isopropyl groups. A figure that includes the H atoms as well as a space-filling diagram is available as Fig. S1 in the Supplementary Material; these show that the As atom in Dipp_3As is effectively hidden from external influence. A survey of the 169 tri-carbon $R_3\text{As}$ structures reported in the Cambridge Structure Database (CSD version 5.34 with updates to February, 2013)^[20] indicates that only Tripp_3As approximates the degree of steric pressure encountered in Dipp_3As . Indeed the next largest values encountered amongst these structures for $\sum \angle \{\text{CAsC}\}$ is in di-*tert*butyl-pentamethyl-cyclopentadien-1-yl-arsenic at 322.4°;^[21] the structure of *tris* (tertbutyl)arsine has apparently not been reported. *Tert*butyl groups induce very large amounts of steric pressure but are relatively poor at shielding.^[17] Another relatively flattened arsenic centre, $\sum \angle \{\text{CAsC}\} = 313.4^\circ$, is encountered in the phosphorus ylide triphenylphosphonium-bis(diphenylarsino)-methylide.^[22] This may be compared with the ‘base’ value in

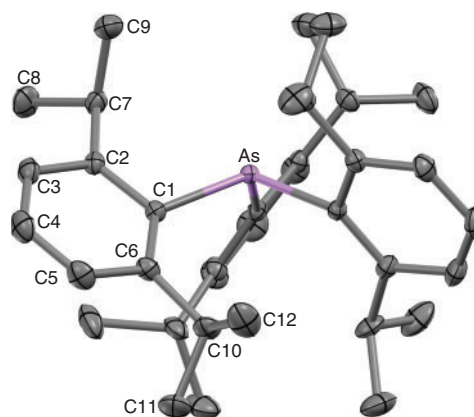


Fig. 1. Displacement ellipsoids plot (30%) of the molecular structure of one enantiomer of Dipp_3As as found in the crystal lattice at 173 K. All three rings are numbered identically due to three-fold rotational crystal symmetry; H atoms omitted for a less obstructed view.

Table 1. Comparative structural data for Dipp_3As and $\text{Dipp}_3\text{As}^{+\bullet}$ from X-ray diffraction and computation^A

Parameter	X-ray diffraction		In R/U-B3LYP/6-31G(d,p)	
	Dipp_3As	$\text{Dipp}_3\text{P}^{\text{B}}$	$\text{Dipp}_3\text{As } C_3$	$\text{Dipp}_3\text{As}^{+\bullet} C_3$
E–C1 [Å]	1.9904(10)	1.8507(16)	2.0136	1.9334
C1–C2 [Å]	1.4179(15)	1.425(2)	1.4252	1.4181
C1–C6 [Å]	1.4050(17)	1.418(2)	1.4152	1.4159
E oop of C1 ^C [Å]	0.656	0.539	0.663	0.174
E oop C2 > C6 ^D [Å]	0.5030(3)	0.430	0.406	0.047
$\sum \angle \{\text{CEC}\}$ [deg.] ^o	329.13	335.64	329.17	357.59
C#1–E–C1 [deg.]	109.71(3)	111.88(5)	109.72	119.20
C2–C6–C1 [deg.]	119.46(11)	118.90(16)	119.31	122.24
C2–C1–As [deg.]	112.16(7)	113.10(12)	112.64	116.56
C6–C1–As [deg.]	127.21(9)	127.17(13)	127.37	121.18

^ASymmetry transformation used to generate equivalent atoms #1 (–y, x – y, z).

^BRef. [1].

^COut of the plane of the three *ipso* C atoms.

^DOut of the plane of the five ring C atoms excluding C1.

tiphenylarsine of $\sum \angle \{CAsC\} = 300.2^\circ$.^[23] Amongst these structures there seem to be an unusually large number of R₃As compounds with strongly pyramidal geometries but bearing substituents that provide a large degree of steric shielding of their HOMOs. Comparative space filling models drawn to scale of 10 contenders for the most sterically shielded R₃As are shown in Fig. S2 in the Supplementary Material alongside similar pictures of Dipp₃As and the ‘base’ compound Ph₃As.^[3,21–29]

Perhaps the most exotic of these species is *tris*((1,2-dicarba-closo-dodecaboran-1-yl)methyl)arsine, in which the central As atom is flanked by three B₁₀C₂ carboranes; this compound

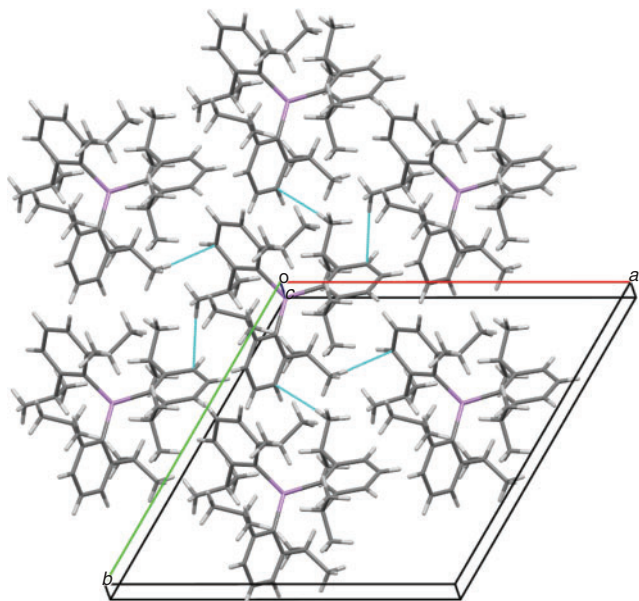


Fig. 2. Packing diagram showing the three-fold symmetry, with dashed lines indicating the only short intermolecular contacts of 2.870(1) Å between isopropyl methyl hydrogen H8C and the π -electron density of ring carbon C3. View is up the *c*-axis.

is reported to react extremely slowly with oxygen.^[24] The other serious contender for highest steric shielding is {1-(8-Me₂N)C₈H₆}₃As which has been shown to display internal coordination between the three pendant dimethylamino groups and the central arsenic atom.^[28] Although this particular compound offers the possibility of electronic as well as steric protection for the HOMO and may thus be especially stable, the relative reactivity of this arsine does not seem to have been further investigated.

Solution Structure by NMR Spectroscopy

The NMR spectra taken in conventional solvents at ambient conditions are consistent with C₃ symmetry (Table 2, with copies of spectra in the Supplementary Material), with all three Dipp groups identical but in the slow-exchange limit for pyramidal inversion. This behaviour is quite different from that of Dipp₃P, which at ambient temperature displays ¹H and ¹³C NMR spectra consistent with D₃ symmetry which is attributed to fast pyramidal inversion.^[1] The latter compound, however, displays spectra at –80°C that fit C₃ symmetry and there is a remarkable similarity between these LT spectra and those of Dipp₃As recorded at RT. This allows assignment of the signals based on those of the phosphine where ³¹P coupling patterns are a helpful aid (Table 2). With reference to the structure shown in Fig. 1 from crystallography, the two isopropyl groups on any of the three rings are shift inequivalent resulting in two methine ¹H resonances at 3.31 and 3.29 ppm. Each isopropyl group also has inequivalent methyl environments resulting in four methyl ¹H doublets of equal intensity (9H each) at 1.28, 1.09, 1.05, and 0.51 ppm. The remarkably high-field resonance of the last listed (assigned to the protons of C12) is caused by ‘anisotropic ring shielding’ from the closer proximity of this particular methyl group to the ring current of an adjacent aromatic ring. The equivalent shift in the LT Dipp₃P spectrum is +0.36 ppm and a reasonable explanation for the differences in chemical shift is a reduced ring shielding influence in the arsine from longer C–As compared with C–P bond lengths. Certainly in the solid

Table 2. ¹H and ¹³C NMR data for Dipp₃As with comparison to Dipp₃P at ambient and low temperature^A

Parameter	C ₁	C ₂	C ₆	C ₄	C ₃	C ₅	C ₁₀	C ₇	C ₉	C ₁₁	C ₈	C ₁₂
Dipp ₃ P ^B												
$\delta(^1\text{H}) + 30^\circ\text{C}^{\text{C}}$				7.29	7.11		3.50		1.17		0.71	
J_{HH} [Hz]				7.68	7.68		6.72		6.72		6.72	
J_{HP} [Hz]				0	3.28		5.20		0		0	
$\delta(^1\text{H}) - 80^\circ\text{C}^{\text{C}}$				7.27	7.07	7.07	3.30	3.14	1.13	0.99	0.90	0.36
J_{HH} [Hz]				7.76	7.58	7.58	~6	~6	6.1	6.3	6.3	6.2
J_{HP} [Hz]				0	3.3	3.3	0	~6.4	0	0	0	0
Dipp ₃ As												
$\delta(^1\text{H}) + 22^\circ\text{C}^{\text{D}}$				7.26	7.04	7.04	3.42	3.28	1.28	1.09	1.05	0.51
J_{HH} [Hz]				7.5	7.5	7.5	6.6	6.6	6.6	6.7	6.7	6.6
Dipp ₃ P ^B												
$\delta(^{13}\text{C}) + 20^\circ\text{C}^{\text{D}}$	135.37	153.64		129.38	124.37		32.37	32.37	23.30			24.82
J_{CP} [Hz]	25.9	18.6		0	3.9		17.6	17.6	0			0
$\delta(^{13}\text{C}) - 80^\circ\text{C}^{\text{C}}$	134.26	153.00	151.94	128.64	125	122.47	32.19	31.40	21.77	22.65	23.59	24.41
J_{CP} [Hz]	25	40	0	0	6	0	0	32	0	0	0	0
Dipp ₃ As												
$\delta(^{13}\text{C}) + 22^\circ\text{C}^{\text{D}}$	139.48	153.67	153.25	129.03	125.31	123.02	33.90	33.02	22.98	24.21	24.45	25.57

^AThe atom numbering scheme is that used in the X-ray structure (Fig. 1) in which all three Dipp rings are identical by symmetry. For H atoms, the attached C atom is designated.

^BFrom Ref. [1].

^CCD₂Cl₂.

^DCDCl₃. Gradient COSY confirms the isopropyl group assignments.

structures, the average methyl-hydrogen to ring-centroid distance is larger in the arsine (C12 to closest ring-centroid distances of 3.81 and 3.77 Å for As and P, respectively).^[1]

The presence of two distinct methine resonances (33.9 and 33.0 ppm) and four different methyl signals at 25.6, 24.5, 24.2 and 23.0 ppm is also observed in the ¹³C NMR spectrum. Moreover, all six phenyl ring carbon resonances are distinct, indicative of frozen or at least slowed rotation about the C_{ipso}-As bond. The signals in Dipp₃As lack the diagnostic presence of phosphorus nuclear couplings and hence the specific assignments in Table 2 are tentative and are based largely on analogy to those obtained in the LT Dipp₃P spectrum. The enforced geometry of these highly sterically encumbered molecules and the excellent fit between the solution NMR and solid-state structural data suggests that the solution structures retain most of the features found in the solid state. That the arsine should still be in the slow exchange limit at RT when the phosphine requires cooling by as much as one hundred degrees to achieve the same state is consistent with estimates of the barriers to pyramidal inversion that are 54–58 kJ mol⁻¹ higher at As compared with P.^[30]

Cyclic Voltammetry (CV) Studies

Dipp₃As was studied by CV on a glassy carbon (GC) electrode in CH₂Cl₂ with 0.4 M [ⁿBu₄N][PF₆] over scan rates of 0.05–20 V s⁻¹ and temperatures of 22 ± 2°C (Table 3). Two oxidation processes appear upon sweeping the potential in the anodic direction from the rest potential, designated as E_p^{a1} and E_p^{a2}. Voltammetric data were calibrated using internal cobaltocenium hexafluorophosphate (i.e. the Cc⁺⁰ redox couple) and expressed on the ferrocene (Fc⁺⁰) scale as zero by subtracting 1.35 V,^[31] and are reported in Table 3. Representative cyclic voltammograms obtained at a scan rate of 0.2 V s⁻¹ are shown in Fig. 3. The first oxidation process displayed close to electrochemically reversible behaviour, with anodic (E_p^{a1}) to cathodic (E_p^{c1}) peak-to-peak separations, ΔE_{p1}, in the range of 119 to 253 mV, and is chemically reversible on the timescale of CV and thus indicative of substantial stability of the cation radical. That this process involves one-electron transfer is evidenced by currents comparable to those from equal molar amounts of internal reference (not shown in the figure) and by the EPR spectroscopic results (see below). The second, irreversible oxidation process labelled E_p^{a2} in Fig. 3 is observed at a considerably more anodic potential, which is similar to what has been reported for Dipp₃P.^[1] For Dipp₃As, fast scanning (up to 20 V s⁻¹) has no effect on the relative size of the return wave for this second process which remains irreversible under all conditions that we studied. Moreover, cycling of the potential through both redox couples serves to decrease the size of the return wave (E_p^{c1}) for the first oxidation process. The I_p^{red}/I_p^{ox} ratio is independent of the scan rate within experimental error for the E_p^{a1}/E_p^{c1} process.

Determination of the Diffusion Coefficients of Dipp₃As

Rotated disk electrode (RDE) measurements on Dipp₃As were undertaken in order to determine the diffusion coefficient *D* by making use of the Levich equation.^[32] Solving for *D* yields an estimate of (3.3 ± 0.1) × 10⁻⁶ cm² s⁻¹ for Dipp₃As. The value for kinematic viscosity (ν_k) was taken to be that of the solvent CH₂Cl₂ at 20°C rather than a measured value for the solution.^[33]

Interpretation of Voltammetric Data

We are aware of only one report that provides comparative redox potential data for numerous triorganoarsines.^[34] Since these authors also report analogous phosphine data, we can

'scale' to the internal Fc⁺⁰ reference scale we established previously for key phosphines (as presented on the right-hand side of Table 4).^[1] The values in Table 4 are therefore directly comparable for all listed species in CH₂Cl₂ solutions; as indicated in the footnotes, the CH₃CN data of Romakhin et al. is also in good agreement with these data since the latter solvent shifts

Table 3. Summary of cyclic voltammetry data obtained for Dipp₃As at a glassy carbon electrode and at T = 22°C

Obtained in CH₂Cl₂ solution containing 0.4 M [ⁿBu₄N][PF₆] measured against (Cc⁺⁰) cobaltocenium redox couple and expressed v. E_{Fc⁺⁰}^o. See text for definition of the parameters described

v [V s ⁻¹]	E _p ^{a1} [V]	E _p ^{c1} [V]	E _{m1} ≅ E _{f1} ^o [V]	ΔE _{p1} [mV]	E _p ^{a2} [V]	I _p ^{red} /I _p ^{ox}
0.05	0.470	0.351	0.410	119	1.402	0.96
0.10	0.470	0.351	0.410	119	1.402	0.91
0.20	0.502	0.354	0.428	148	1.447	0.93
0.40	0.534	0.330	0.432	204	1.514	1.00
0.80	0.565	0.312	0.438	253	1.565	0.98

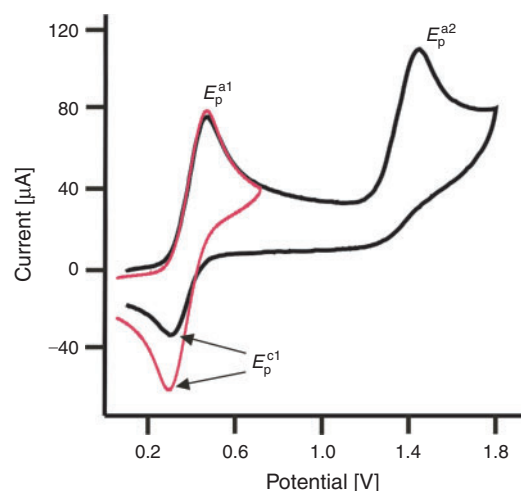


Fig. 3. Cyclic voltammetry of Dipp₃As (5 mM) in CH₂Cl₂ solution containing 0.4 M [ⁿBu₄N][PF₆] under an atmosphere of dry argon at a scan rate of 0.2 V s⁻¹ on a glassy carbon electrode at 22°C: (a) through the first oxidation process (red line), and (b) through the first and second oxidation processes (black line).

Table 4. Comparative redox potential data in CH₂Cl₂ for R₃E (E = As, P)^A

See text for definition of the parameters listed

Compound	E _{m1} ≅ E _{f1} ^o [V]	Compound	E _{m1} ≅ E _{f1} ^o [V]	ΔE _{m1} s	Δ[∑∠{CEC}] _{P→As}
Ph ₃ As ^{B,C}	(0.96)	Ph ₃ P ^E	(0.88)	0.08	7.9 ^F
Mes ₃ As ^{B,D}	0.51	Mes ₃ P ^E	0.19	0.32	6.3 ^F
Dipp ₃ As	0.42	Dipp ₃ P ^E	0.09	0.33	6.5 ^F
Tripp ₃ As ^B	0.28	Tripp ₃ P ^E	-0.06	0.34	6.7 ^F

^AMidpoint potentials from cyclic voltammetry or rotated disk electrode (RDE) measurements, scan rate = 0.2 V s⁻¹; values in parenthesis are E^{ox} peak potentials.

^BRef. [2], corrected by -0.22 V based on Mes₃P potentials, see Ref. [1].

^C+1.11 V in CH₃CN, Ref. [34].

^D+0.62 V in CH₃CN, Ref. [34].

^ERef. [1].

^FFrom the published crystal structures and this work; see also Ref. [17].

phosphine oxidation potentials +0.07–0.10 V more positive.^[1] If we disregard the Ph₃E species, since for such irreversible redox processes the potentials may be strongly affected by the rates of follow-up reactions, for the other three species with reversible or close-to-reversible behaviour we find that corresponding arsines are +0.32 to +0.34 V more difficult to oxidise than phosphines. This is fully consistent with lower-lying HOMOs as a result of the more pyramidal geometry at the central atom. The structural studies already discussed inform us that the change for Ar₃E from P to As results in a decrease in the sum of angles around the pnictogen of 6.3°–6.7° (Table 4) for the three with reversible E_{m1} values.

Fluid Solution EPR Characterisation of Dipp₃As^{+•}

The chemically reversible Dipp₃As^{+•/0} redox couple occurs at an average potential of +0.43 V v. Fc^{0/+}, and no further oxidation occurs under CV conditions until +1.45 V v. Fc^{0/+} (with onset of current flow for this second process >1.2 V). The list of potential chemical oxidising agents provided by Connelly and Geiger advises that the Ag^I ion in CH₂Cl₂ solution should be a suitable oxidant for one-electron oxidation, with little chance of initiating double oxidation to the presumably unstable dication (the Ag^{+•/0} redox couple is reported as +0.65 V v. Fc^{0/+} in this solvent).^[35] This is an attractive reagent because the by-product is expected to precipitate as solid silver. Therefore AgPF₆ was used to generate solutions of [Dipp₃As]^{+•} PF₆⁻ salts in CH₂Cl₂.

Oxidised solutions prepared under vacuum in sealed tubes subsequent to freeze–thaw degassing of the solvent displayed persistent fluid solution EPR spectra (Fig. 4a). Based on experience with corresponding phosphines and evidence from density functional theory (DFT) calculations (see below), the dominant hyperfine coupling is expected to be from the single arsenic nucleus (⁷⁵As, $I = 3/2$, 100% abundant), which ought to result in a four-line spectrum with equal spacing and a 1 : 1 : 1 : 1

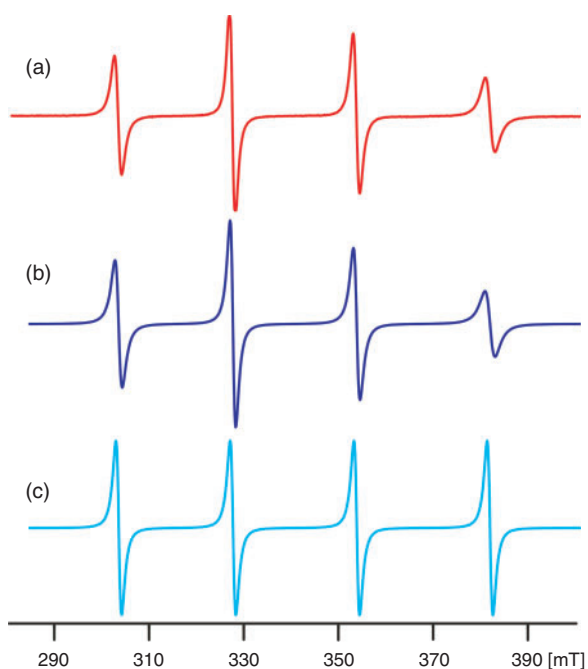


Fig. 4. (a) Experimental fluid solution EPR spectrum of Dipp₃As^{+•} obtained after chemical oxidation determined at 293 K. (b) Best simulated spectrum (third-order perturbation theory and line-widths corrected for tumbling). (c) Simulation as in (b) without the tumbling correction.

intensity ratio. However, what is observed are four lines with different intensities *and* different spacing.

The unequal intensity pattern is a consequence of ‘slowed tumbling’ from incomplete averaging of the g and a tensors.^[36] This partial averaging of the signals can be accounted for by a linear fit to the correlation time for molecular motion which accurately fits the peak-to-peak line widths ΔB_{p-p} to three constants A , B , and C (Table 5). The unequal spacing of the lines is a consequence of the large size of the ⁷⁵As hyperfine splitting (on the order of 26 mT, ~8% of the resonant field strength); when the energy of the hyperfine interaction approaches that of the Zeeman interaction the two are not fully separable. This is commonly referred to as a ‘higher order’ interaction, since an accurate solution to the spin Hamiltonian by perturbation methods requires second or third order terms.^[37] Importantly, the magnitude of both the hyperfine coupling and the Zeeman energy are affected, and hence a full simulation is required to recover both the a and g terms accurately. The effects of the two corrections are illustrated by the full lineshape simulations shown in Fig. 4. Fig. 4b incorporates both corrections while Fig. 4c shows the corrected line positions but has the linewidth correction turned off so as to better illustrate the separate effects.

Excellent agreement with the experimental spectrum is thereby achieved and the corrected a and g values are presented in Table 5. At 293 K, $a(^{75}\text{As}) = 26.1$ mT and $g = 2.045$. There is significant temperature dependence of the EPR linewidth parameters consistent with slowed re-orientational motion on cooling. Such a dependence has been observed previously for Dipp₃P^{+•} (R. T. Boéré, Y. Zhang, unpubl. data). In their preliminary report, Sasaki et al. did not comment on temperature dependence for Tripp₃As^{+•},^[2] but the published ambient temperature spectrum indicates that this radical is also in the slowed tumbling regime; they report a g -value of 2.042 (which would appear *not* to have been corrected for the higher-order coupling) and an apparent isotropic $a(^{75}\text{As})$ of 26.4 mT. These authors also report EPR data for Mes₃As^{+•} of $g = 2.038$ and $a(^{75}\text{As}) = 27.5$ mT but here too it is not clear if the appropriate corrections were made.

Frozen Solution EPR Characterisation of Dipp₃As^{+•}

In frozen CH₂Cl₂ solutions at 183 K, a characteristic axially symmetric powder pattern was obtained for Dipp₃As^{+•} with

Table 5. Fluid solution EPR data for Dipp₃As^{+•} from full lineshape simulations^A

See text for definition of the parameters listed

Temp. [K]	g -value	$a(^{75}\text{As})$ [mT]	A^B [mT]	B^B [mT]	C^B [mT]
293	2.0210	26.11 ^C	1.30	−0.16	0.24
273	2.0210	26.20	1.45	−0.23	0.36
263	2.0210	26.20	1.74	−0.34	0.55
243	2.0220	26.25	2.03	−0.42	0.75
233	2.0220	26.25	2.36	−0.53	0.97

^ASimulations undertaken with *SimFonia*, v. 1.26 (Bruker Biospin, 1996).

^BLinewidth parameters A , B , and C determined from the simulations by fitting to $\Delta B_{p-p} = A + Bm_1 + Cm_2^2$. A , B , and C depend linearly on the correlation time and on the anisotropic a and g tensors. A and C are always positive, while B can be positive or negative and determines which line is broadened most in the spectrum, Ref. [36]. For a plot of the A constant v. temperature, see Fig. S5 in the Supplementary Material.

^CFrom the simulation; measured spacings of the lines at 293 K: 24.126, 26.136, and 28.272 mT.

parallel and perpendicular hyperfine splitting (HFS) tensor components of 47.9 and 19.0 mT (Fig. 5a). The parallel and perpendicular g tensors are almost the same, so the EPR spectrum is close to being a g -isotropic system ($g_{\parallel} = 2.000$ mT and $g_{\perp} = 2.003$ mT). The simulation achieved is in reasonable agreement with the observed spectrum and the fit is extremely sensitive to alteration of the parameters (Fig. 5b). There is a paucity of comparative data for triorgano-arsoniumyl radical cations in the literature but what we have been able to locate is presented in Table 6. There seems to be only a single report about $\text{Ph}_3\text{As}^{+\bullet}$, in which it was produced by radiolysis in sulfuric acid.^[38] By contrast, when Ph_3As reacts with oxygen-based free radicals, adducts of the type $\text{Ph}_3\text{As-OR}^{\bullet}$ are the major products.^[39,40] Two studies on $\text{Mes}_3\text{As}^{+\bullet}$ report somewhat divergent parameters.^[2,41] The values of a_{\parallel} and a_{\perp} allow for the calculation of the relative s and p spin densities at As using the

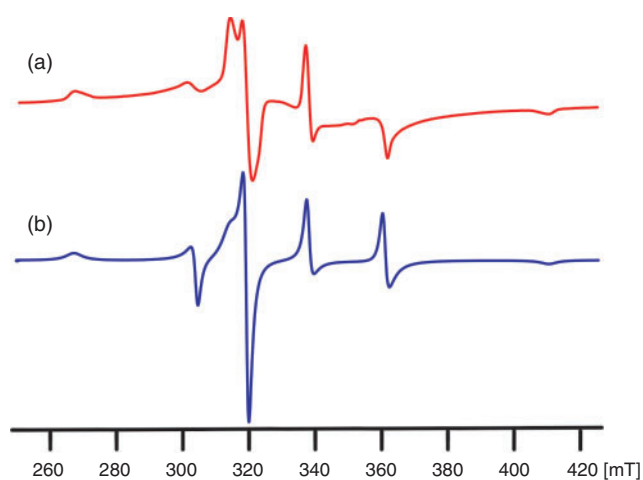


Fig. 5. (a) Experimental frozen solution EPR spectrum of $\text{Dipp}_3\text{As}^{+\bullet}$ obtained by chemical oxidation in CH_2Cl_2 at 183 K and (b) simulation obtained using second order perturbation theory (line width (LW) for the simulation $x = y = 1.5$; $z = 3.5$ mT).

calculated full-spin hyperfine parameters of Morton and Preston.^[37,42] From this value the Coulson equation permits an estimation of the pyramidal character of the radical cations (further details on this procedure are found in the Supplementary Material).^[43] As expected, $\text{Dipp}_3\text{As}^{+\bullet}$ is greatly flattened upon oxidation (a change in $\sum \angle \{\text{CAsC}\}$ of 22° from that in the neutral molecule). This parameter is only marginally smaller in $\text{Mes}_3\text{As}^{+\bullet}$ (using the Il'yasov data) but $\text{Ph}_3\text{As}^{+\bullet}$ is, as expected, noticeably more pyramidal.^[7,8]

DFT Calculations on $\text{Dipp}_3\text{As}^{+\bullet/0}$

DFT calculations were undertaken in order to obtain information about the structure of the radical cation as well as to gain insights into the changes in electronic structure that accompany the oxidation of Dipp_3As (details of methodology and atom coordinates are provided in the Supplementary Material.) Only the neutral and +1 oxidation state have been considered as we yet have little experimental evidence about a putative dication; if in fact $\text{Dipp}_3\text{As}^{2+}$ is formed at the potential of the second observed CV peak, it would seem to be very electrophilic and is destroyed by adventitious moisture or by other pathways. However, the radical cation is persistent and solutions prepared under vacuum last for days or more. For neutral Dipp_3As the agreement between the calculated and experimental X-ray geometry (Table 1) is excellent. Key strained bond distances agree within 1% and angles within 0.5%. The calculated and experimental $\sum \angle \{\text{CAsC}\}$ is identical within experimental error. The most significant deviation occurs in the amount by which the As atom lies above the plane of the five non-*ipso* phenyl ring C atoms; the gas-phase calculation predicts less distortion from ideality than the solid state structure.

This agreement provides some confidence in assessing the (unknown) radical structure. The Coulson equation provides an estimate of $\sum \angle \{\text{CAsC}\} = 351.0^\circ$ for $\text{Dipp}_3\text{As}^{+\bullet}$ from the EPR data (Table 6). The DFT calculated value is even more planar at 357.6° . Three crystal structures recently reported for $\text{Tripp}_3\text{P}^{+\bullet}\text{X}^-$ salts have measured $\sum \angle \{\text{CPC}\}$ ranging from 359.64° to 359.99° .^[9] These authors also report that their DFT

Table 6. EPR and structural parameters in $\text{Dipp}_3\text{As}^{+\bullet}$ and related radicals

See text for definition of the parameters listed

Species	g_{iso}	g_{\parallel}	g_{\perp}	a_{iso} [mT]	a_{\parallel} [mT]	a_{\perp} [mT]	ρ_{4p}/ρ_{4s}	$\sum \angle \{\text{CAsC}\}$ [deg.]	$\sum \angle \{\text{CAsC}\}_{\text{DFT}}$ [deg.]
$\text{Dipp}_3\text{As}^{+\bullet\text{A}}$	2.021	2.000	2.003	26.1	47.9	19.0	14.8	351.0	357.6
$\text{Tripp}_3\text{As}^{+\bullet\text{B}}$	2.042	2.002	2.020	26.4	48.3	19.25	14.7	350.9	–
$\text{Mes}_3\text{As}^{+\bullet\text{B}}$	2.038	2.004	2.056	27.5	45.6	17.7	15.1	351.2	–
$\text{Mes}_3\text{As}^{+\bullet\text{C}}$	2.016	1.96	2.044	27.9	46.2	19.3	13.9	350.5	–
$\text{Ph}_3\text{As}^{+\bullet\text{D}}$	<i>2.070</i>	1.995	2.017	<i>30.9</i>	46.5	23.1	11.1	348.4	–

^AThis work; 183 K.

^BRef. [2]; the magnitude of the g factors suggest that the parameters are uncorrected for second order effects.

^CRef. [42].

^DRef. [39]; frozen solution 77 K; italicized isotropic values are calculated from the anisotropic data.

Table 7. Summary of density functional theory calculations for $\text{Dipp}_3\text{E}^{+\bullet/0}$ (E = P, As)^A

See text for definition of the parameters listed

Species	$\sum \angle \{\text{CEC}\}$ (neutral) [deg.]	$\sum \angle \{\text{CEC}\}$ (cation) [deg.]	$\Delta \sum \angle \{\text{CEC}\}$ [deg.]	Exp a_{iso} [mT]	Calc a_{iso} [mT]	ρ_{E}
Dipp_3As	329.17	357.6	28.4	26.1	18.7	0.787
$\text{Dipp}_3\text{P}^{[1]}$	336.6	359.7	23.1	23.9	13.4	0.858

^AR/U B3LYP/631G(d,p) density functional theory calculations using *Gaussian 03W* (full details in the Supplementary Material).

calculations on Dipp₃P^{+•} only converge when planarity is imposed. We found no difficulty in optimising the non-planar Dipp₃As^{+•} structure which is confirmed by a frequency calculation. As Pan et al. also conclude, the bending mode for flattening this class of radical cation with highly congested substituents is probably very small.^[9] Nevertheless the substantial size of the HFS values measured for such R₃E^{+•} species, whether E is As or P, strongly supports solution-phase structures that have minima with pyramidal geometries and indeed substantial lifetimes in these pyramidal states, however low the barrier to pyramidal inversion may be.

The calculated spin density on P in Dipp₃P^{+•} is 0.858 (Table 7), compared with 0.787 on As in Dipp₃As^{+•} (the remaining spin density is distributed over the C and H atoms, which contributes significantly to line broadening) (R. T. Boeré, Y. Zhang, unpubl. data). The ratio of the solution phase isotropic HFS of 23.9 mT in Dipp₃P and 26.1 mT in Dipp₃As, is 0.916. The ratio of the calculated full-spin hyperfine parameters A_{iso} for ³¹P and ⁷⁵As of 474.79 and 523.11 mT is 0.908.^[37,42] The similarity in these values also suggests that the amount of s-orbital spin density on Dipp₃P^{+•} and Dipp₃As^{+•} is more congruent than indicated by the (relatively low-level) DFT calculations.

Experimental

Materials and General Methods

Unless otherwise stated, all work was carried out under a dry nitrogen atmosphere, using standard Schlenk techniques or an MBraun Glove box. AsCl₃ (Aldrich) was used as received. Magnesium turnings (Aldrich) were stored in a glove box and activated by grinding before use. Solvents for synthesis were collected from a solvent purification system (MBraun) or distilled under an N₂ atmosphere and degassed by freeze–pump–thaw degassing. Drying agents for solvent purification include sodium/benzophenone (tetrahydrofuran) and sodium (*n*-heptane). ¹H and ¹³C NMR spectra were recorded on a Bruker/Tecmag AC250 spectrometer (¹H, 250.13 MHz; ¹³C, 62.9 MHz) and referenced relative to 0 ppm for tetramethylsilane (¹H, ¹³C) using either deuterated chloroform or deuterated benzene as secondary references. Electrospray ionisation (ESI) mass spectra were measured using a Thermo Instruments Exactive *orbitrap* spectrometer. For the electrochemical experiments, dichloromethane (BDH, reagent grade) was purified by distillation from CaH₂ and was purged with dry argon before use. Electrochemical grade tetra-*n*-butylammonium hexafluorophosphate [ⁿBu₄N][PF₆] (Fluka) was used as the supporting electrolyte and was kept in a desiccator before use. Bis(cyclopentadienyl)cobalt(III) hexafluorophosphate (Aldrich) was used as the potential reference.

Preparation of Dipp₃As

Activated (grinding and heating in vacuum) magnesium turnings (0.56 g, 22.5 mmol), dibromoethane (0.1 mL), and tetrahydrofuran (20 mL) were heated at reflux for 30 min. To the cooled mixture, DippBr (5.41 g, 22.5 mmol) was added, followed by vigorous stirring and heating at reflux for 2.5 h. The mixture was then stirred overnight at RT. The resultant solution of DippMgBr^[44] was cooled to –70°C and CuCl (98%, 2.40 g, 23.8 mmol) was added followed by stirring for 1 h at –70°C, and then warmed to RT and shielded from direct light. AsCl₃ (98%, 1.19 g, 6.44 mmol) was added and the mixture was stirred for 30 min at –70°C, warmed to RT and heated to reflux overnight, and then cooled to RT. Precipitated CuCl was removed by

filtration under vacuum. Thin layer chromatography (TLC) of the tan coloured residue after solvent removal indicated two components. Column chromatography on silica with hexanes eluted the leading band, which was recovered and recrystallised from hot *n*-heptane to afford crystalline Dipp₃As (1.59 g, 2.76 mmol, 43% yield), mp 339–345°C, determined to be pure by NMR spectroscopy. A second crystallisation from *n*-heptane afforded blocks suitable for X-ray diffraction. For NMR data see Table 2. *m/z* (ESI, CH₃CN) Calc. for C₃₆H₅₁As (M^{+•}) 558.32012. Found 558.31885. Anal. Calc. for C₃₆H₅₁As: C 77.39, H 9.20. Found: C 77.41, H 9.23%.

X-Ray Crystallographic Study

A colourless prism of Dipp₃As (0.24 × 0.18 × 0.15 mm³) was coated in Paratone oil, mounted on a glass fibre, and cooled to –100°C for data collection on a Bruker Apex II CCD area detector diffractometer (MoK_{α1}, λ 0.71073 Å) using ω–φ scans (θ range = 2.45° to 28.81°), followed by data correction and reduction using *SAINTE-Plus*.^[45] A total of 9509 reflections were measured of which 2635 were unique (R_{int} 0.05). The structure was solved with dual-space methods (*SHELX-M*) and refined with *SHELX-L*.^[46] The compound, C₃₆H₅₁As, formula weight 558.69, was found to crystallise in the hexagonal space group R3 (#146) [*a* 16.6193(16) Å, *c* 10.1772(16) Å], with three molecules per unit cell. A semi-empirical absorption correction (*SADABS*) from equivalents was applied ($\mu = 0.14 \text{ mm}^{-1}$, transmission factors 0.856 and 0.784).^[45] The data is complete (99.9%) down to 0.77 Å; R_1 0.0494, wR_2 0.1138 for 2635 observed data and a goodness of fit (GOF) of 1.064, with largest peaks and hole in the final difference map of 0.29 and –0.28 e Å^{–3}. In the course of refinement the distribution of intensity data was found not to match that expected for this chiral space group. Subsequently, the structure was successfully refined as a racemic twin (twinning by merohedry) in a 61 : 39 ratio. *Mercury 3.1* was employed for crystallographic figures and post-refinement data analysis.^[47] CCDC 937361 contains the supplementary crystallographic data for this paper. These data can be obtained free of charge from The Cambridge Crystallographic Data Centre via www.ccdc.cam.ac.uk/data_request/cif.

Cyclic Voltammetry

Cyclic voltammograms were obtained at room temperature in CH₂Cl₂ containing 0.4 M [ⁿBu₄N][PF₆] as the supporting electrolyte. These solutions were purged with dry argon for 10 min directly before use, and argon gas flowed over the solutions during experiments. The cell design utilised a conventional three electrode setup with a 3.0 mm diameter GC working electrode, a Pt wire auxiliary and a silver wire quasi-reference electrode. The working electrode was polished with a 0.3 micron Al₂O₃ (Buehler, 0.05 μm) slurry on a clean polishing cloth, rinsed with distilled water and acetone, and dried with tissue paper before use. The reference electrode was separated from the bulk solution by a fine porosity frit. Experiments commenced with initial background scans to characterise the size of the electrochemical window and provide an estimate of the likely background current. Cyclic voltammograms were obtained over scan rates of 0.050–20 V s^{–1}. All potentials are reported versus the operative formal potential, $E_{\text{Fc}^{+0}}$, for the Fc⁺⁰ redox couple. The Cc⁺⁰ (Cc = cobaltocene) redox couple is known to appear at –1.35 V in CH₂Cl₂; data have been converted into the Fc⁺⁰ scale by subtraction of 1.35 V.^[31]

RDE Voltammetry

RDE voltammetry measurements on CH_2Cl_2 solutions 5.73 mM in Dipp_3As were performed on a Princeton Applied Research PARSTAT 2273 potentiostat in conjunction with a PINE Model AFMSRXE Modulated Speed Rotator. The cell used for RDE measurements replaced the central size-10 joint with a 60 mm \times 15 mm cylinder to accommodate the rotating electrode. A 5.0 mm diameter GC macrodisc electrode (area = $1.86 \times 10^{-1} \text{ cm}^2$) was employed for RDE measurements. Diffusion coefficients were determined from the limiting current values obtained from RDE voltammetry and use of the Levich equation.^[32] The value for kinematic viscosity (ν_k) was taken to be that of the solvent CH_2Cl_2 at 20°C, $0.003318 \text{ cm}^2 \text{ s}^{-1}$.^[33] Rotation rates from 1000 to 2250 rpm were applied over a potential range of -0.5 to $+1$ V. Plots of the limiting current (I_L) v. the square root of the rotational velocity ($\omega^{-1/2}$) yielded a straight line with slope = $(0.62nFAC\nu^{-1/6}D^{2/3})^{-1}$ (where n is the number of electrons in the charge-transfer process, F is the Faraday constant, A is the electrode area (cm^2), C is the concentration (mol cm^{-3}), and D is the diffusion coefficient). Solving for D yields an estimate of $3.3 \pm 0.1 \times 10^{-6} \text{ cm}^2 \text{ s}^{-1}$ for Dipp_3As .

EPR Spectroscopic Studies of Chemically Oxidized $\text{Dipp}_3\text{As}^{\bullet+}$

An excess of AgPF_6 was added to solid Dipp_3As in a 'T' cell consisting of a 4 mm Pyrex EPR tube fused at a 75° angle to an 8 mm Pyrex reaction tube. Dry degassed CH_2Cl_2 was vacuum distilled onto the solid mixture in the reaction tube and the tube was flame sealed. Upon melting, an immediate colour change was observed. The concentration of radical in the EPR tube was controlled by internal distillation of the solvent so that the effects of concentration broadening on the EPR linewidths could be monitored. All spectra were obtained on a Bruker EMX Plus/10 instrument operating at X band frequencies (9.8 GHz) and variable temperature (VT) experiments were performed using the ER4141 VT accessory. Modulation amplitude was varied between 1 to 5 G to optimize signal to noise for each experiment and the sweep width was varied between 150 and 300 mT.

Supplementary Material

Full crystallographic data with comparison to the Dipp_3P structure; supplementary crystallographic figure; figure of space filling models showing steric shielding in R_3As structures; ^1H and ^{13}C NMR spectra for Dipp_3As ; EPR linewidth temperature dependence plot; use of the Coulson equation; and DFT computational results and references are available on the Journal's website.

Acknowledgements

The authors thank the University of Lethbridge and the Natural Sciences and Engineering Research Council of Canada for financial support of this work. The diffractometer was purchased with the help of both these agencies. The EPR and mass spectrometers were purchased with support from the Canada Foundation for Innovation, the Government of Alberta, Bruker Canada, Ltd (EPR) and Thermo Fisher Canada Inc. (mass spectrometry).

References

- [1] R. T. Boéré, A. M. Bond, S. Cronin, N. W. Duffy, P. Hazendonk, J. D. Masuda, K. Pollard, T. L. Roemmele, P. Tran, Y. Zhang, *New J. Chem.* **2008**, 32, 214. doi:10.1039/B709602J
- [2] S. Sasaki, K. Sutoh, F. Murakami, M. Yoshifuji, *J. Am. Chem. Soc.* **2002**, 124, 14830. doi:10.1021/JA027493N
- [3] S. Sasaki, F. Murakami, M. Yoshifuji, *Organometallics* **2006**, 25, 140. doi:10.1021/OM050522T
- [4] S. Sasaki, M. Yoshifuji, *Curr. Org. Chem.* **2007**, 11, 17. doi:10.2174/138527207779316507
- [5] S. Sasaki, R. Chowdhury, M. Yoshifuji, *Tetrahedron Lett.* **2004**, 45, 9193. doi:10.1016/J.TETLET.2004.10.084
- [6] F. Chaliér, Y. Berchadsky, J. Finet, G. Gronchi, S. Marque, P. Tordo, *J. Phys. Chem.* **1996**, 100, 4323. doi:10.1021/JP952854P
- [7] C. Palau, Y. Berchadsky, F. Chaliér, J. Finet, G. Gronchi, P. Tordo, *J. Phys. Chem.* **1995**, 99, 158. doi:10.1021/J100001A028
- [8] M. Culcasi, Y. Berchadsky, G. Gronchi, P. Tordo, *J. Org. Chem.* **1991**, 56, 3537. doi:10.1021/JO00011A018
- [9] X. Pan, X. Chen, T. Li, Y. Li, X. Wang, *J. Am. Chem. Soc.* **2013**, 135, 3414. doi:10.1021/JA4012113
- [10] R. T. Boéré, *Electron Paramag. Reson.* **2013**, 23, 22. doi:10.1039/9781849734837-00022
- [11] D. Martin, M. Soleilhavoup, G. Bertrand, *Chem. Sci.* **2011**, 2, 389. doi:10.1039/C0SC00388C
- [12] J. Konu, T. Chivers, in *Stable Radicals: Fundamentals and Applied Aspects of Odd-Electron Compounds* (Ed. R. G. Hicks) **2010**, pp. 381–406 (John Wiley: Chichester).
- [13] A. Armstrong, T. Chivers, R. T. Boéré, *ACS Symp. Ser.* **2006**, 917, 66. doi:10.1021/BK-2005-0917.CH005
- [14] S. Marque, P. Tordo, *Top. Curr. Chem.* **2005**, 250, 43.
- [15] P. P. Power, *Chem. Rev.* **2003**, 103, 789. doi:10.1021/CR020406P
- [16] M. Geoffroy, *Recent Res. Dev. Phys. Chem.* **1998**, 2, 311.
- [17] R. T. Boéré, Y. Zhang, *J. Organomet. Chem.* **2005**, 690, 2651. doi:10.1016/J.JORGANCHEM.2004.11.043
- [18] F. J. Brady, C. J. Cardin, D. J. Cardin, D. J. Wilcock, *Inorg. Chim. Acta* **2000**, 298, 1. doi:10.1016/S0020-1693(99)00343-6
- [19] B. Twamley, C.-S. Hwang, N. J. Hardman, P. P. Power, *J. Organomet. Chem.* **2000**, 609, 152. doi:10.1016/S0022-328X(00)00162-5
- [20] F. H. Allen, *Acta Crystallogr.* **2002**, B58, 380.
- [21] P. Jutzi, S. Pilotek, B. Neumann, H.-G. Stammer, *J. Organomet. Chem.* **1998**, 552, 221. doi:10.1016/S0022-328X(97)00588-3
- [22] H. Schmidbaur, P. Nussstein, G. Muller, *Z. Naturforsch. B: Chem. Sci.* **1984**, 39, 1456.
- [23] A. N. Sobolev, V. K. Belsky, N. Yu. Chernikova, F. Yu. Akhmadulina, *J. Organomet. Chem.* **1983**, 244, 129. doi:10.1016/S0022-328X(00)98593-0
- [24] A. S. King, G. Ferguson, J. F. Britten, J. F. Valliant, *Inorg. Chem.* **2004**, 43, 3507. doi:10.1021/IC0499471
- [25] O. bin Shawkataly, I. A. Khan, C. S. Yeap, H.-K. Fun, *Acta Crystallogr.* **2009**, E65, o2772.
- [26] S. C. Chmely, T. P. Hanusa, A. L. Rheingold, *Organometallics* **2010**, 29, 5551. doi:10.1021/OM100474M
- [27] H. Lang, L. Zsolnai, *Z. Naturforsch. B: Chem. Sci.* **1990**, 45, 1529.
- [28] S. Kamepalli, C. J. Carmalt, R. D. Culp, A. H. Cowley, R. A. Jones, N. C. Norman, *Inorg. Chem.* **1996**, 35, 6179. doi:10.1021/IC960516C
- [29] A. N. Sobolev, I. P. Romm, N. Yu. Chernikova, V. K. Belsky, E. N. Guryanova, *J. Organomet. Chem.* **1981**, 219, 35. doi:10.1016/0022-328X(81)85007-3
- [30] J. D. Andose, A. Rauk, K. Mislow, *J. Am. Chem. Soc.* **1974**, 96, 6904. doi:10.1021/JA00829A016
- [31] R. S. Stojanovic, A. M. Bond, *Anal. Chem.* **1993**, 65, 56. doi:10.1021/AC00049A012
- [32] A. J. Bard, L. R. Faulkner, *Electrochemical Methods: Fundamentals and Applications, 2nd edn* **2001** (John Wiley & Sons: New York, NY).
- [33] J. Nath, A. P. Dixit, *J. Chem. Eng. Data* **1984**, 29, 317. doi:10.1021/JE00037A027
- [34] A. S. Romakhin, E. V. Nikitin, O. V. Parakin, Y. A. Ignat'ev, B. S. Mironov, Y. M. Kargin, *J. Gen. Chem. U.S.S.R.* **1987**, 2298.
- [35] N. G. Connelly, W. E. Geiger, *Chem. Rev.* **1996**, 96, 877. doi:10.1021/CR940053X
- [36] D. M. Murphy, in *Metal Oxide Catalysis* (Eds S. D. Jackson, J. S. J. Hargreaves) **2009**, Vol. 1, pp. 1–50 (Wiley-VCH: Weinheim).

- [37] J. A. Weil, J. R. Bolton, J. E. Wertz, *Electron Paramagnetic Resonance: Elementary Theory and Practical Applications*, 2nd edn **1994** (John Wiley & Sons: New York, NY).
- [38] G. W. Eastland, M. C. R. Symons, *J. Chem. Soc. Perkin* **1977**, II, 833.
- [39] E. Furimsky, J. A. Howard, J. R. Morton, *J. Am. Chem. Soc.* **1972**, *94*, 5932. doi:10.1021/JA00771A088
- [40] E. Furimsky, J. A. Howard, J. R. Morton, *J. Am. Chem. Soc.* **1973**, *95*, 6574. doi:10.1021/JA00801A009
- [41] A. V. Il'yasov, Y. M. Kargin, E. V. Nikitin, A. A. Vafina, G. V. Romanov, O. V. Parakin, A. A. Kazakova, A. N. Pudovik, *Phosphorus Sulfur* **1980**, *8*, 259. doi:10.1080/03086648008078199
- [42] J. R. Morton, K. F. Preston, *J. Magn. Reson.* **1978**, *30*, 577.
- [43] C. A. Coulson, in *Volume Commémoratif Victor Henri, Contributions à l'Etude de la Structure Moléculaire* **1948**, pp. 12–32 (Desoer: Liège).
- [44] R. R. Schrock, M. Wesolek, A. H. Liu, K. C. Wallace, J. C. Dewan, *Inorg. Chem.* **1988**, *27*, 2050. doi:10.1021/IC00285A012
- [45] *APEX2, SAINT-Plus and SADABS* **2008** (Bruker AXS Inc.: Madison, WI).
- [46] G. M. Sheldrick, *Acta Crystallogr.* **2008**, *A64*, 112.
- [47] C. F. Macrae, I. J. Bruno, J. A. Chisholm, P. R. Edgington, P. McCabe, E. Pidcock, L. Rodriguez-Monge, R. Taylor, J. van de Streek, P. A. Wood, *J. Appl. Cryst.* **2008**, *41*, 466. doi:10.1107/S0021889807067908